Interaction between nearest equivalent magnetic ions in neighboring unit cells result from linkages of the type:

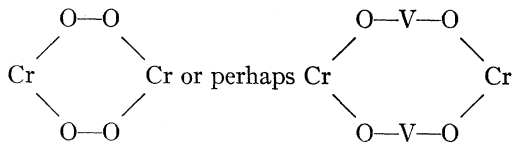

These are found to be ferromagnetic in all cases as they must be if the magnetic cell is to be identical with the chemical cell. Thus, while a single type of interaction for a path through only one tetrahedral group does not occur, when two such paths are available, a consistent ferromagnetic interaction results.

ACKNOWLEDGMENTS

The authors wish to thank Dr. R. Nathans, Dr. S. J. Pickart, and Dr. F. Stern for helpful discussions of the results. They also acknowledge the valuable assistance of Mr. Ronald Horwath in the preparation of samples and associated x-ray studies.

PHYSICAL REVIEW VOLUME 125, NUMBER 4 FEBRUARY 15, 1962

Reflectivity of Gray Tin Single Crystals in the Fundamental Absorption Region

MANUEL CARDONA AND D. L. GREENAWAY
Laboratories RCA Ltd., *Zurich, Switzerland*
(Received October 2, 1961)

Single crystals of gray tin have been grown by the method of Ewald from a mercury solution. The reflection coefficient of a surface of growth has been measured in the fundamental absorption region. The reflectivity shows two maxima as in other semiconductors with diamond and zinc-blende structure. The lower energy maximum exhibits a doublet structure. The energy at which this maximum occurs is interpreted as the energy gap at the L point of the Brillouin zone. The energy separation of the doublet components gives the spin-orbit splitting of the valence band at the L point. From the measured value of the L gap the transverse effective mass at the bottom of the conduction band is estimated to be 0.06 m. Several general conclusions about the systematics of the band structure in all semiconductors with diamond and zinc-blende structure are presented.

I. INTRODUCTION

A. Semiconducting Properties of Gray Tin

THE semiconducting character of gray tin was established in 1950 by several authors[1] from electrical measurements on polycrystalline material. Extensive studies of the galvanomagnetic properties of gray tin were performed by Busch and Wieland[2] and Kohnke and Ewald.[3] From these measurements, a value of 0.08 ev for the thermal energy gap at 0°K was obtained. The complete interpretation of these experimental results, especially the derivation of the free carrier mobilities, concentrations, and effective masses, was very difficult since conventional semiconductor techniques such as optical absorption, drift mobility, and cyclotron resonance measurements could not be applied to the polycrystalline samples available. The diamagnetic susceptibility of intrinsic and doped polycrystalline samples was studied by Busch and Moser.[4] By combining these measurements with the galvanomagnetic measurements and with a number of additional assumptions, the free carrier mobilities, effective masses, and concentrations were estimated. Photoconductivity measurements on polycrystalline gray tin films were performed by Becker[5] at 4°K. The estimate of the energy gap obtained from these measurements (0.075 ev) is somewhat uncertain. The results of these measurements have been reviewed by Busch and Kern in a recent article.[6]

In 1958 Ewald and Tufte[7] succeeded in preparing gray tin single crystals from a saturated mercury solution at −30°C. Galvanomagnetic measurements on samples from these single crystals were performed by Tufte and Ewald.[8] The magnetoresistance exhibited an anisotropy attributed to the electrons and corresponding to conduction-band minima along the [111] direction. The anisotropy ratio K (equal to the effective-mass anisotropy ratio divided by the scattering-time anisotropy ratio) was shown to be greater than 2.3 at room temperature. At low temperature (77°K) no magnetoresistance anisotropy was observed. This fact was attributed to the anisotropy of the ionized impurity scattering which compensates the effective mass

[1] A. Blum and N. A. Gorynuova, Doklady Akad. Nauk SSSR **75**, 367 (1950); G. Busch, J. Wieland, and H. Zoller, Helv. Phys. Acta **23**, 528 (1950); J. T. Kendall, Proc. Phys. Soc. (London) **B63**, 821 (1950).
[2] G. Busch and J. Wieland, Helv. Phys. Acta **26**, 697 (1953).
[3] E. E. Kohnke and A. W. Ewald, Phys. Rev. **102**, 1481 (1956).
[4] G. Busch and E. Moser, Helv. Phys. Acta **26**, 611 (1953).
[5] J. H. Becker, thesis, Cornell University, 1957 (unpublished).
[6] G. Busch and R. Kern, *Solid-State Physics*, edited by F. Seitz and D. Turnbull (Academic Press, Inc., New York, 1960), Vol. 11, p. 1.
[7] A. W. Ewald and O. N. Tufte, J. Appl. Phys. **29**, 1007 (1958).
[8] O. N. Tufte and A. W. Ewald, Phys. Rev. **122**, 1431 (1961).

anisotropy. No optical measurements on gray tin single crystals have been reported.

B. Fundamental Reflectivity of Semiconductors with Diamond and Zinc-Blende Structure

The reflectivity of semiconductors with diamond and zinc-blende structure has recently received considerable attention. Philipp and Taft,[9] Tauc and Antoncik,[10] and Cardona and Sommers[11] have studied the reflectivity of germanium. The reflectivity of silicon has been discussed by Philipp and Taft,[12] Tauc and Abraham,[3] and Cardona.[14] The reflectivity of the III-V compounds has been studied by Tauc and Abraham[13] and Cardona[14] and the reflectivity of the II-VI compounds by Cardona[14] and by Aven, Marple, and Segall.[15] All these reflectivity spectra show a striking similarity. Two reflectivity maxima are present in all materials studied. With the exception of silicon and GaP, the low energy maximum always exhibits a doublet structure. This doublet is produced by an absorption edge which is not seen in the conventional transmission measurements since it corresponds to much higher absorption coefficients than the fundamental absorption edge. However, transmission measurements showing these strong absorption edges have been made by Cardona and Harbeke[16] on evaporated layers of the II-VI compounds. These absorption edges are probably produced by allowed transitions between the valence and the conduction band at the L point of k space (edge of the Brillouin zone in the [111] direction). The reasons for this identification have been discussed by Cardona and Sommers.[11] The doublet structure of the corresponding reflectivity maxima is due to the spin-orbit splitting of the valence band at the L point.

Since attempts to transmit light through a gray tin single crystal have been unsuccessful,[6] it was felt that the reflectivity techniques would provide unambiguous information about the band structure of gray tin. Such measurements are reported in this paper and compared with similar measurements in other semiconductors with diamond and zinc-blende structure.

II. METHOD OF MEASUREMENT

A. Equipment

The reflectivity of several gray tin samples was measured by comparison with the reflectivity of a previously calibrated aluminum mirror. The radiation produced by a tungsten bulb or a hydrogen arc was passed through a Bausch and Lomb monochromator and detected by a Mullard 61SV PbS photocell or an RCA 936 photoemissive cell. The sample was placed inside a cryostat with a quartz window, and nearly normal incidence ($i<10°$) used. At each wavelength, the light intensity reflected by the sample and by the standard mirror were measured successively in order to avoid the error produced by slow changes in source intensity.

B. Sample Preparation

Gray tin single crystals were grown by the method of Ewald and Tufte.[7] The white tin used as a starting material was obtained from Johnson, Matthey & Company, London, and had a purity better than 99.999%. The growth apparatus contained 2 kg of mercury and dissolved tin at a rate of 2.5 g per day. The crystals used in the measurements were obtained after 2, 3, and 4 weeks operation. Only crystals with at least one perfect surface were used and mercury, which wetted this surface after taking the crystal out of the growth apparatus, was removed (with the help of a Q tip) at a temperature slightly above the melting point of mercury. The reflectivity measurements were performed directly on the surfaces of growth without any further treatment. The sample area available for the reflectivity measurements was of the order of 5 mm^2.

III. RESULTS

The reflectivity spectrum of 5 gray tin single crystals was measured for photon energies between 0.8 and 4.8 ev. Figure 1 shows the spectrum obtained for a typical sample at 200°K. A reflectivity doublet is seen with components at 1.29 and 1.73 ev and another maximum at 3.65 ev. The reflectivity spectrum of the other samples measured differs slightly from the one shown in Fig. 1, but the same structure is observed for all samples and the position of the maxima is always the same within the experimental error. The average values obtained for the energy of the doublet components are 1.755 ± 0.02 ev, 1.28 ± 0.02 ev, and for the higher energy maximum 3.66 ± 0.02 ev. The average values of the energy separation between the doublet components is 0.475 ± 0.03 ev.

IV. DISCUSSION

A. Interpretation of the Reflectivity Peaks

The reflectivity spectrum shown in Fig. 1 is very similar to the spectrum observed for all other materials with diamond and zinc-blende structure.[10,11,13,14] In these materials, the reflectivity doublet has been interpreted as due to direct electronic transitions between the valence and the conduction band at the L point of the Brillouin zone. The energy E_1 of the strongest component of the doublet corresponds to

[9] H. R. Philipp and E. A. Taft, Phys. Rev. **113**, 1002 (1959).
[10] J. Tauc and E. Antoncik, Phys. Rev. Letters **5**, 253 (1960).
[11] M. Cardona and H. S. Sommers, Jr., Phys. Rev. **122**, 1382 (1961).
[12] H. R. Philipp and E. A. Taft, Phys. Rev. **120**, 37 (1960).
[13] J. Tauc and A. Abraham, *Proceedings of the International Conference on Semiconductor Physics, Prague, 1960* (Czechoslovakian Academy of Sciences, Prague, 1961), p. 375.
[14] M. Cardona, J. Appl. Phys. **32**, 2151 (1961).
[15] M. Aven, D. T. F. Marple, and B. Segall, J. Appl. Phys. **32**, 2261 (1961).
[16] M. Cardona and G. Harbeke, Phys. Rev. Letters (to be published).

the vertical energy gap at the L point. The high energy reflectivity maximum has been tentatively attributed by Phillips[17] to direct transitions between the valence and the conduction band at the X point of the Brillouin zone ([100] direction, edge of the zone). This interpretation is questionable since the X_1 conduction band point is doubly degenerate only when the crystal has inversion symmetry and should split for the crystals without center of symmetry. No splitting of the corresponding reflectivity maximum has been observed for the III-V and II-VI compounds. Table I shows the thermal gap E_0, the position of the low-energy component of the reflectivity doublet E_1, the temperature coefficient of E_1, the position of the high-energy reflectivity maximum E_2, the experimentally determined spin-orbit splitting of the valence band at the center of the Brillouin zone Δ_0(exp), the splitting of the reflectivity doublet Δ_1(exp), and the estimated value of the spin-orbit splitting of the valence band at the L point Δ_1(calc). When no reference is given, the values are those reported in this paper or in reference 14. The spin-orbit splitting in gray tin was estimated from the atomic spin-orbit splitting (0.81 ev) by assuming that the atomic splittings in germanium (0.35 ev) and gray tin are proportional to the splittings in the crystal. The agreement between the value of Δ_1(calc) and Δ_1(exp) makes it also reasonable to assign the reflectivity doublet in gray tin to direct transitions at the L point. The small systematic deviation between the estimated and observed splittings could be corrected by slightly adjusting the proportionality constant between atomic and crystal splittings.

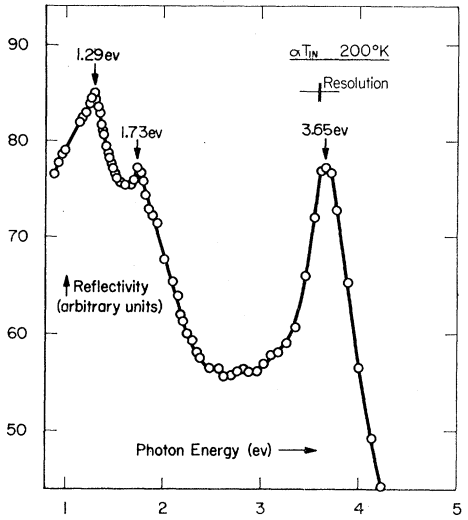

FIG. 1. Reflectivity of single-crystal gray tin at 200°K.

B. Effective Masses at the L Point

From the measured value of the L gap in gray tin, it is possible to estimate the transverse effective masses of the conduction and valence bands by using Kane's $\mathbf{k}\cdot\mathbf{p}$ perturbation method.[18] Ehrenreich[19] has shown that the electron effective masses m_e found for germanium and the III-V compounds at $k=0$ are given by the formula:

$$\frac{m}{m_e}=1+\frac{E_p}{E_g}\left(\frac{2}{3}+\frac{1}{3}\frac{E_g}{E_g+\Delta_0}\right), \tag{1}$$

TABLE I. Optical gap (E_0), energies of the reflectivity peaks (E_1 and E_2), temperature coefficient of E_1, measured spin-orbit splittings of the valence band at the Γ point [Δ_0(exp)] and at the L point [Δ_1(exp)], and estimated values of the spin-orbit splittings at the L point [Δ_1(calc)] for several semiconductors with diamond and zinc-blende structure.

Material	E_0(ev) 297°K	E_1(ev) 297°K	$(dE_1/dT)\times10^4$ ev(°C)$^{-1}$	E_2(ev) 297°K	Δ_0(exp)	Δ_1(exp)	Δ_1(calc)
α-Sn	0.08(0°K)	1.28(200°K)	···	3.5	···	0.47	0.42
Ge	0.67	2.10	−(4.2±0.4)	4.45	0.30	0.18	0.18
Si	1.10	3.38	−(2.7±0.6)	4.4	···	···	0.03
InSb[a]	0.18	1.82	···	4.13	···	0.56	0.48
InAs[a]	0.33	2.52	···	4.72	0.43[b]	0.29	0.27
GaSb	0.70	2.02	−(4.2±0.6)	4.3	···	0.46	0.42
GaAs[a]	1.35	2.94	···	5.1	0.33[b]	0.26	0.22
InP	1.26	3.15	−(4.2±0.6)	5.0	···	0.14	0.13
AlSb	1.6	2.78	−(5.0±1)	···	0.75[c]	0.40	0.38
GaP	2.24	3.71	−(2.5±0.6)	···	···	···	0.07
HgTe	0.02	2.08	···	4.70	···	0.69	0.73
CdTe	1.5	3.29	···	···	···	0.55	0.64
ZnTe	2.1	3.57	−(5.0±0.6)	···	···	0.56	0.62
HgSe	0.6	2.82	−(4.3±0.6)	···	···	0.31	0.41
ZnSe	2.67	4.75[d]	···	6.4[d]	0.43	0.35[d]	0.31
ZnS	3.6	5.52[e]	···	···	···	···	0.07

[a] See reference 13.
[b] R. Braunstein, J. Phys. Chem. Solids **8**, 280 (1959).
[c] W. J. Turner and W. E. Reese, Phys. Rev. **117**, 1003 (1960).
[d] See reference 15.
[e] C. K. Coogan, Proc. Phys. Soc. (London) **70**, 845 (1957).

[17] J. C. Phillips, J. Phys. Chem. Solids **12**, 208 (1960).
[18] E. O. Kane, J. Phys. Chem. Solids **1**, 249 (1957).
[19] H. E. Ehrenreich, J. Appl. Phys. **32**, 2155 (1961).

which is obtained from Kane's theory by considering only the interaction between the lowest conduction band and the highest valence band. E_g is the energy gap at $k=0$ and E_p is proportional to the square of a matrix element of the linear momentum and equal to 20 ev for all these materials. With the same assumptions (see Appendix) one finds for the transverse effective masses at the L_1 conduction band minimum and at the L_4^- and L_6^- valence-band maxima into which the L_3' maximum splits by spin-orbit interaction:

$$\frac{m}{m_\perp^*(L_1)}=1+\frac{E_p}{E_1+\Delta_1/2},$$
$$\frac{m}{m_\perp^*(L_4^-)}=-1+\frac{E_p}{2E_1}, \qquad (2)$$
$$\frac{m}{m_\perp^*(L_6^-)}=-1+\frac{E_p}{2(E_1+\Delta_1)}.$$

From the value of $m(L_1)=0.081m$ found by Fletcher *et al.*[20] for germanium, one finds $E_p=25$ ev and, by using Eq. (2), one gets for gray tin:

$$m_\perp^*(L_1)=0.057m, \quad m_\perp^*(L_4^-)=0.11m,$$
$$m_\perp^*(L_6^-)=0.15m. \qquad (3)$$

The same method can be applied to estimate the effective masses at the L point for all other semiconductors of Table I, except for silicon, GaP, and ZnS where Eq. (2) has to be modified to take into account the fact that the lowest L conduction band minimum probably has L_3 symmetry.[14] The method gives no information about the longitudinal masses since the [111] component of the linear momentum has no matrix element between the L_1 and L_3' states.

It has been shown by Tufte and Ewald[8] that at room temperature the electrons in gray tin belong mostly to conduction band minima centered along the [111] direction of k space. Measurements of the conductivity as a function of pressure[21] yield a pressure coefficient of the thermal gap, $dE_0/dp=\pm 5\times 10^{-6}$ ev cm^2/kg, indicating that the lowest conduction band minima have L_1 symmetry[22] in agreement with Tufte and Ewald's results. Hence $m_\perp^*(L_1)$ is the transverse effective mass at the bottom of the conduction band in gray tin.

The average electron-hole density of states effective mass $(m_{ed}^* m_{hd}^*)^{\frac{1}{2}}$ can be determined if the electron and hole concentrations, n and p are known as a function of temperature by means of the formula:

$$np=2.33\times 10^{31}\left(\frac{m_{ed}^* m_{hd}^*}{m^2}\right)^{\frac{3}{2}} \nu e^{-\beta/k} e^{-E_0/kT} T^3, \qquad (4)$$

where ν is the number of equivalent conduction band minima (4 for gray tin), E_0 the thermal gap at 0°K, and β the temperature coefficient of this gap. Kohnke and Ewald[3] determined the product np as a function of temperature from conductivity and Hall data assuming that the free carrier mobilities obey a power law as a function of temperature and that this law is the same for the electrons in gray tin as in n-type germanium. They found from Eq. (4) $(m_{ed}^* m_{hd}^*)^{\frac{1}{2}}=0.68m$ by taking $\nu=1$ and $\beta=-5\times 10^{-5}$ ev (°C)$^{-1}$. Although the value of β has not been directly measured for gray tin, all semiconductors of this family have values of β around -4×10^{-4} ev (°C)$^{-1}$. Kohnke and Ewald's results yield for $\beta=-4\times 10^{-4}$ ev (°C)$^{-1}$ and $\nu=4$, $m_{ed}^* m_{hd}^*=0.01m^2$. By extrapolating the known values of the hole effective masses in germanium and silicon one can estimate for gray tin $m_{hd}^*\approx 0.2m$. This gives

$$m_{ed}^*=m_\perp^*(L_1)^{\frac{2}{3}} m_{\|}^*(L_1)^{\frac{1}{3}}=0.05m.$$

By taking $m_{\|}^*(L_1)\approx 1$ and $m_\perp^*=0.057m$, we obtain $m_{ed}^*\approx 0.15m$ which compares with the value quoted above.

Better agreement with our estimate of $m^*(L_1)$ is obtained by using the values of np found from magnetic susceptibility measurements by Busch and Moser.[4] Taking $\nu=4$ and $\beta=-4\times 10^4$ ev (°C)$^{-1}$, we obtain from these data $m_{ed}^*=0.13m$ for $m_{hd}^*=0.2m$ which is in good agreement with our estimate. These authors also measured the diamagnetic susceptibility of n- and p-type doped material. From these measurements they found $m_h^*=0.21m$, in good agreement with our estimate, and for the electrons the average effective mass

$$\left[\frac{1}{3m^*(L_1)}\left(\frac{2}{m_{\|}(L_1)}+\frac{1}{m_\perp(L_1)}\right)\right]^{-\frac{1}{2}}=0.16m,$$

also in good agreement with the value $0.1m$ obtained from $m_{\|}^*(L_1)=m$ and $m_\perp^*(L_1)=0.057$m.

Lindquist and Ewald[23] found from infrared reflectivity measurements an average electron and hole effective mass equal to $0.10m$ which agrees well with the value 0.09 m estimated from our data.

TABLE II. Energy difference between the top of the valence band at Γ and L for some group IV and III-V semiconductors.

	$E(L_1)-E(\Gamma_{25'}$ or $\Gamma_4)$	E_1	$E(\Gamma_{25'}$ or $\Gamma_4)-E(L_{3'}$ or $L_3)$
Ge	0.62	2.10	1.48
Si			1.30[a]
Sn	0	1.28	1.28
GaSb	0.81[b]	2.02	1.21
GaAs	1.7[c]	2.94	1.24
InSb	0.45[d]	1.82	1.37
InAs	1.0[e]	2.53	1.53

[a] See reference 24.
[b] M. Cardona, J. Phys. Chem. Solids **17**, 336 (1961).
[c] H. Ehrenreich, Phys. Rev. **120**, 1951 (1960).
[d] J. C. Woolley, C. M. Gillett, and J. A. Evans, J. Phys. Chem. Solids **16**, 138 (1960).
[e] J. C. Woolley (private communication).

[20] R. C. Fletcher, W. A. Yager, and F. R. Merrit, Phys. Rev. **100**, 747 (1955).
[21] S. Groves and W. Paul (private communication).
[22] W. Paul, J. Phys. Chem. Solids **8**, 196 (1959).
[23] A. W. Ewald (private communication).

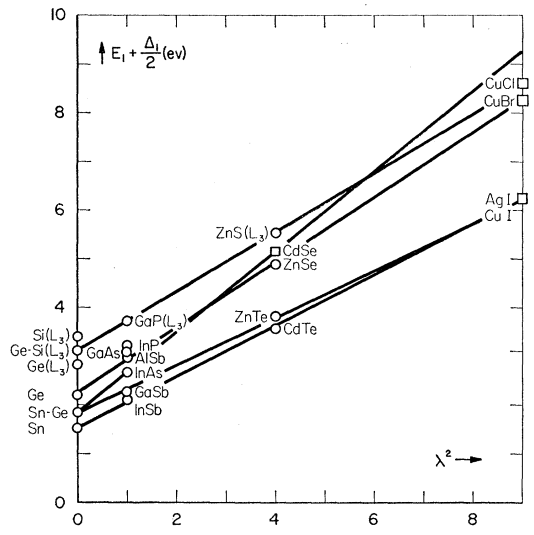

FIG. 2. $E_1+\Delta_1/2$ as a function of perturbation coefficient for several isoelectronic semiconductor sequences (○ measured points; □ estimated).

C. General

Table II lists for some semiconductors the room temperature energy difference between the L_1 conduction band state and the top of the valence band state ($\Gamma_{25'}$ or Γ_4 depending on whether there is a center of symmetry or not), and the value of the E_1 gap given in Table I. The difference between these values gives the energy separation between the top of the valence band at Γ and at L. The value of this separation in silicon has been determined by Tauc and Abraham.[24] In spite of large differences in the band structure of the 5 materials listed, $E(\Gamma_{25'}$ or $\Gamma_4)-E(L_{3'}$ or $L_3)$ is always about 1.35 ev. It has been shown moreover by Herman[25] that this energy is very insensitive to changes in the core energy shifts. It is also easy to show that this energy is not affected by the spin-orbit interaction (see Appendix). If we postulate that this energy is about 1.35 ± 0.15 ev for all semiconductors of the same family, the position of the lowest L conduction band minimum with respect to the top of the valence band can be estimated for other materials of the same family by means of the expression $E(L_1)-E(\Gamma_{25'}$ or $\Gamma_4)=E_1-1.35$ ev.

A semiempirical method has been proposed by Herman[26] to correlate the gaps of semiconductors of the same isoelectronic sequence. The crystal potential for any group IV, III-V, II-VI, or I-VII semiconductor with diamond or zinc-blende structure is written as

$$V=V^{\mathrm{IV}}_{\mathrm{sym}}+V^{\mathrm{IV}}_{\mathrm{antisym}}+\lambda(V^{\mathrm{polar}}_{\mathrm{sym}}+V^{\mathrm{polar}}_{\mathrm{antisym}}), \qquad (5)$$

where $V^{\mathrm{IV}}_{\mathrm{sym}}$ and $V^{\mathrm{IV}}_{\mathrm{antisym}}$ are the symmetrical and antisymmetrical components of the crystal potential of the corresponding isoelectronic group IV element. $V^{\mathrm{IV}}_{\mathrm{antisym}}$ is zero for the horizontal sequences (Sn, InSb, CdTe, AgI; Ge, GaAs, ZnSe, CuBr). The term in brackets in Eq. (5) is a perturbation potential. The coefficient λ represents the strength of the perturbation and is taken equal to 1, 2, and 3 for the III-V, II-VI, and I-VII compounds, respectively. The effect of the symmetric part of the perturbation is in general much smaller than that of the antisymmetric part and will be neglected. The expectation values of $V^{\mathrm{polar}}_{\mathrm{antisym}}$ at the L point are zero when the corresponding group IV semiconductor has inversion symmetry, that is, when the sequence is horizontal. In this case $V^{\mathrm{polar}}_{\mathrm{antisym}}$ produces an increase in the energy gap with increasing λ in second-order perturbation theory. This increase will thus be proportional to λ^2. Figure 2 shows the energy gap without the spin-orbit perturbation $E_1+\Delta_1/2$ (see Appendix) as a function of λ^2. The λ^2 proportionality of $E_1+\Delta_1/2$ holds not only for the horizontal sequences but also for the skew sequences (Sn-Ge, GaSb, ZnTe) provided that one takes for the gap of the group IV element the average gap of the two components.

For the skew sequence Ge-Si, GaP, ZnS we have assumed that the L conduction-band minimum has L_3 symmetry[14] as in silicon and taken the position of the L_3 conduction-band minimum in germanium given by Tauc and Abraham.[24] This sequence also obeys the λ^2 law. The InP and AlSb points fall close to the line of the corresponding horizontal isoelectronic sequence (Ge, GaAs, ZnSe). The perturbation is higher for the InAs and InP skew sequences than for the GaSb and AlSb sequences. Figure 2 enables us to predict the value of $E_1+\Delta_1/2$ for a number of materials where it has not yet been observed. A similar estimate can be made for the position of the high energy reflectivity peak E_2 if we assume the λ^2 law also holds. The values of $E_1+\Delta_1/2$ and E_2 estimated for several materials are listed in Table III.

Note added in proof. After submitting this article a doublet structure has been seen at the E_2 reflectivity peak of GaAs, ZnSe,[27] and InAs.[28] Therefore, the interpretation of this peak in terms of $X_4\rightarrow X_1$ transitions is confirmed. The E_1 peak in Si, GaP, and ZnS seems

TABLE III. Estimates of $E_1+\Delta_1/2$ and E_2 for some materials where no experimental values are available.

	CdTe	CdSe	ZnTe	ZnSe	AgI	CuI	CuBr	CuCl
$E_1+\Delta_1/2$	···	5.2	···	···	6.2	6.2	8.3	8.6
E_2	5.8	6.6	5.1	···	8.8	6.5	9.0	···

[24] J. Tauc and A. Abraham, J. Phys. Chem. Solids **20**, 190 (1961).
[25] F. Herman, *Proceedings of the International Conference on Semiconductor Physics, Prague, 1960* (Czechoslovakian Academy of Sciences, Prague, 1961), p. 20
[26] F. Herman, J. Electronics **1**, 103 (1955).
[27] H. Ehrenreich, H. R. Phillipp, and J. C. Phillips, Phys. Rev. Letters **8**, 59 (1952).
[28] D. Greenaway (unpublished).

due to $\Gamma_{25'} \rightarrow \Gamma_{15}$ transitions[27] and not to $L_{3'} \rightarrow L_3$ as stated tentatively in this paper. The structure seen in gray tin around 2.8 ev (see Fig. 1) may also be due to these transitions. The $L_{3'} \rightarrow L_3$ transitions seem to be responsible for the structure observed in the reflectivity of germanium and silicon around 5.5 ev.[27] We have seen some structure in the reflectivity of gray tin at 4.4 ev which is probably also due to the $L_{3'} \rightarrow L_3$ transitions.

ACKNOWLEDGMENTS

We wish to acknowledge the help of Heinrich Meier in growing the gray tin crystals. Thanks are also due to Dr. A. W. Ewald and Dr. Rudolf Nitsche for advice in the crystal growth and Dr. William Paul and Dr. Steven Groves for discussions.

APPENDIX

The energy levels in gray tin around the L point are given by the eigenvalues of the Hamiltonian[18] H:

$$H-\hbar^2k^2/2m=H_0+\hbar\mathbf{k}\cdot\mathbf{p}/m + (\hbar/4m^2c^2)[\nabla V\times\mathbf{p}]\cdot\boldsymbol{\sigma}, \quad \text{(A1)}$$

where H_0 is a k-independent Hamiltonian, p is the linear momentum operator, V is the crystal potential, and the components of $\boldsymbol{\sigma}$ are the spin matrices. The k-dependent spin-orbit splitting has been neglected and the origin of k space is taken to be the L point. If we only consider the interaction between the L_1 conduction band and the $L_{3'}$ valence band, with respect to the basis

$$|S\uparrow\rangle,\quad |x\uparrow\rangle,\quad |y\uparrow\rangle,\quad |S\downarrow\rangle,\quad |x\downarrow\rangle,\quad |y\downarrow\rangle.$$

($|S\uparrow\rangle$ is invariant under the group of the k vector at L, and $|x\uparrow\rangle$ and $|y\uparrow\rangle$ transform like x and y, respectively. The arrows indicate whether the spin is up or down); $H-\hbar^2k^2/2m$ is given by

$$\begin{vmatrix} H_1 & 0 \\ 0 & H_2 \end{vmatrix}, \quad \text{(A2)}$$

where

$$H_1=\begin{vmatrix} E_s & Pk_x & 0 \\ Pk_x & 0 & \Delta/3 \\ 0 & \Delta/3 & 0 \end{vmatrix} \quad H_2=\begin{vmatrix} E_s & Pk_x & 0 \\ Pk_x & 0 & -\Delta/3 \\ 0 & -\Delta/3 & 0 \end{vmatrix},$$

$$P=-(\hbar/m)\langle S|p_x|x\rangle,$$

$$\Delta=\left(3\hbar i/4mc^2\right)\left\langle x\left|\frac{\partial V}{\partial x}p_y-\frac{\partial V}{\partial y}p_x\right|y\right\rangle.$$

In Eq. (A2) we have taken $k_y=k_z=0$ since we are only interested in the transverse effective masses. The origin of energy is the top of the valence band for the unperturbed Hamiltonian H_0. The eigenvalues of Eq. (A2) are given by the roots α of the cubic secular equation:

$$(E_s-\alpha)(\alpha^2-\Delta^2/9)+P^2k_x^2\alpha=0, \quad \text{(A3)}$$

which for $k_x=0$ become

$$\begin{aligned} &\alpha=E_s && \text{(conduction band)},\\ &\alpha=+\Delta/3 && \text{(valence band } L_6^-),\\ &\alpha=-\Delta/3 && \text{(valence band } L_4^-). \end{aligned} \quad \text{(A4)}$$

The spin-orbit splitting of $L_{3'}$ is $2\Delta/3$. The value of the splitting at the Γ point is Δ,[18] evaluated at this point. Since Table I shows that for a number of materials $\Delta_1=\frac{2}{3}\Delta_0$, we conclude that the matrix element Δ is about the same regardless of whether we evaluate it at Γ or at L. We have shown in Sec. IV that the same applies to the matrix element P. The top of the valence band at L is raised by an amount $\Delta/3$ by the spin-orbit interaction. The same also happens to the valence band at Γ,[18] thus we conclude that the energy separation between the top of the valence band at Γ and at L is left unaltered by the spin-orbit interaction.

The following expression for the transverse effective masses at L_1, L_4^-, and L_6^- is found by differentiating Eq. (A3):

$$\frac{m}{m_\perp}=1+\frac{2}{\hbar^2}\frac{dE}{d(k^2)}=1-\frac{2P^2\alpha}{2\hbar^2\alpha(E_s-\alpha)-(\alpha^2-\Delta^2/9)\hbar^2}. \quad \text{(A5)}$$

Substituting Eq. (A4) into Eq. (A5), Eqs. (2) are found for the conduction and valence band transverse effective masses at the L point.